

WHIRC Report IV-- Ghost Images II

Dick Joyce
8 August 2008

Introduction

During the night of 15 July 2008, we repeated the observations of a heavily saturated star in a more systematic manner than in the observations of 15 April 2008 reported earlier to investigate ghost image and scattering artifacts as a function of both wavelength and field position.

- The star α Ser ($J = 0.83$; $H = 0.29$; $K = 0.15$) was imaged with an integration time of 5 s, sufficient to saturate the peak by a factor $\sim 10^4$.
- Images were taken in the J, H, and Ks filters at positions: on-axis, 50S, 50W50S, and 75W75S.
- Additional images at Ks were obtained along the array diagonal at 15W15S, 30W30S, 45W45S, and 60W60S to investigate an interesting scattered light artifact.

Analysis

The conditions were reasonably clear, but not photometric. Because of the weather conditions and the bright artifacts, it was not possible to generate sky images for subtraction. Since the sky, even at Ks, was negligible compared to the primary star, this should not affect the analysis. Image FWHM ranged from 0.59 (J) to 0.48 (Ks) arcsec.

A field star ($J = 10.00$; $H = 9.40$; $K = 9.35$) located 24W and 52N of α Ser provided a useful unsaturated calibration for normalizing the flux of the saturated primary star. The images were normalized so the calculated *peak* of the α Ser image was 1.0.

This analysis is more systematic than that carried out on the 15 April 2008 data and this report should be considered to supersede the conclusions reached in the earlier report. In particular, the ghost labeled 'A' in the earlier report is likely an afterimage from the previous image. Such an afterimage was seen in the second image taken in the current series, at the position of the star in the first image, where it had been illuminating the array for several minutes. To avoid confusion, the same nomenclature for the ghosts will be employed here.

The images (displayed on a logarithmic scale to enhance the appearance of the faint ghosts) are presented below. Contour plots of the four H band images are also shown. *Because of the limited capability of the contour routine, it was necessary to block average the images by a factor of 8 before making the contour maps. The 128×128 plots therefore cover 1024×1024 pixels on the image. While enhancing the low surface brightness artifacts, this process makes the two compact ghosts more difficult to see on the contour plots.*

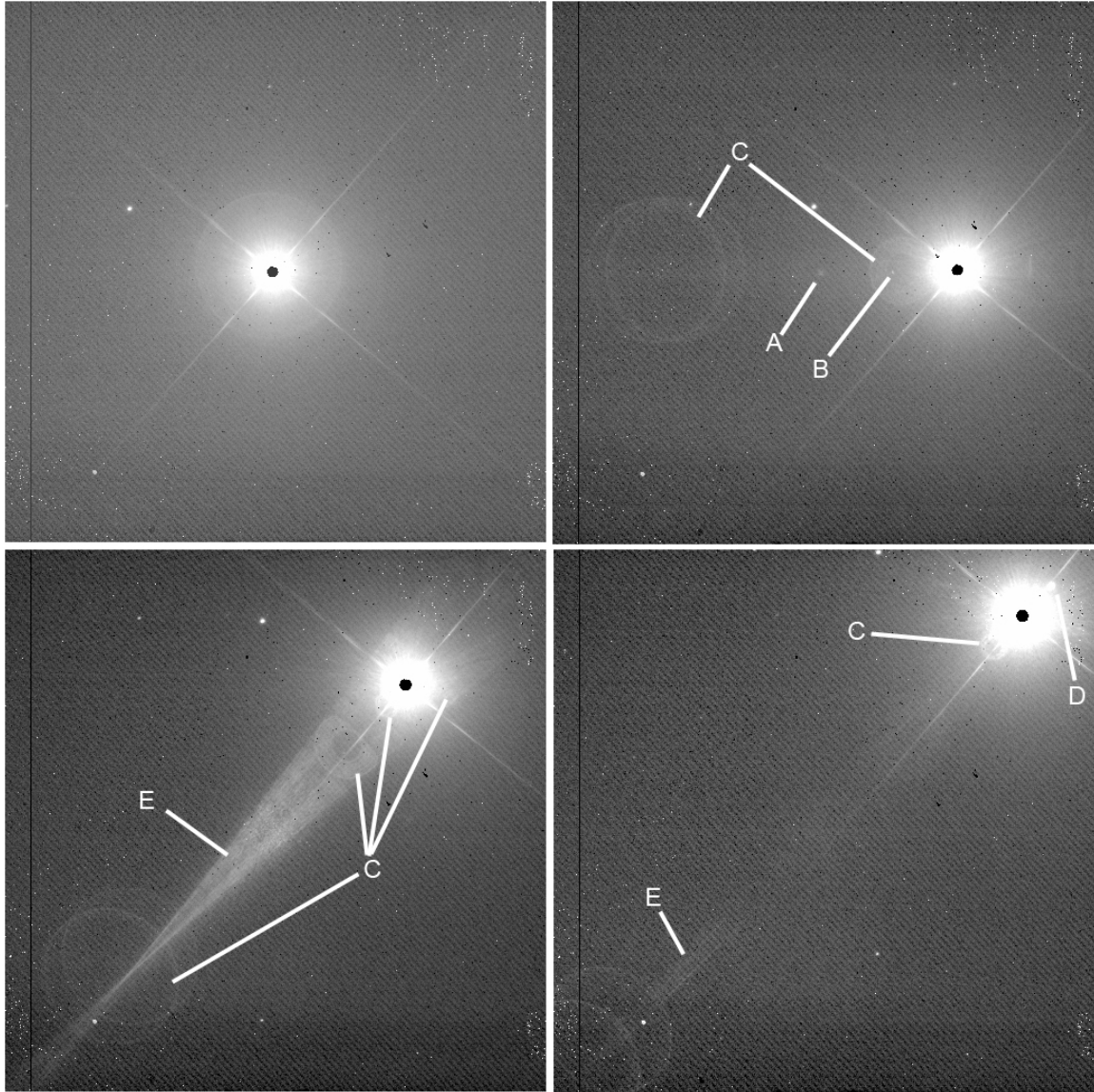


Figure 1: Images of α Ser in the J band on-axis (upper left), 50S (upper right), 50W50S (lower left) and 75W75S (lower right). The various ghosts, described in the text, are marked. Ghost 'A', which was seen only in this one image, is not a ghost, but an afterimage of the star in the on-axis frame, where it had remained on the array for several minutes.

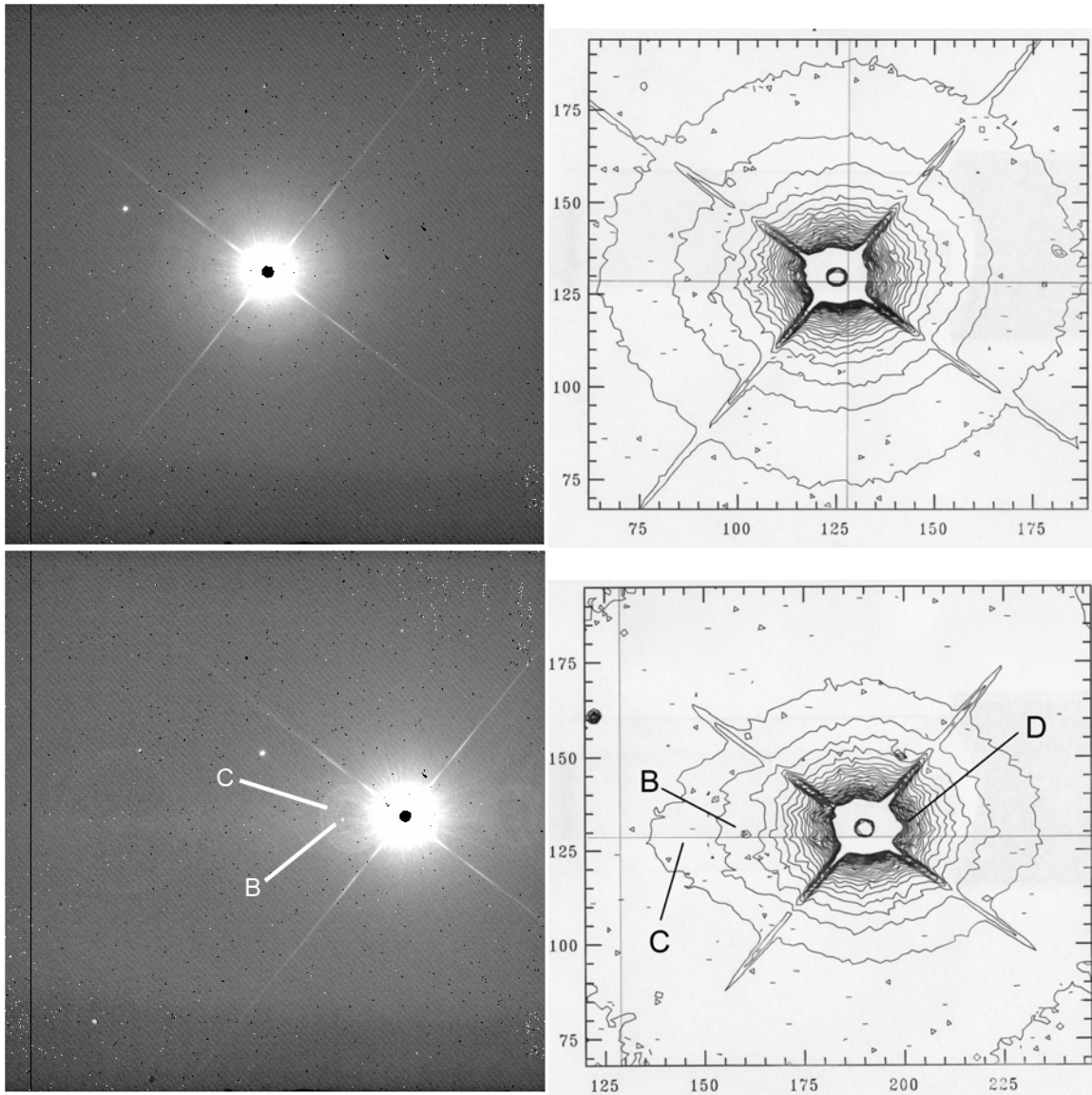


Figure 2: Images of α Ser in the H band on-axis (upper left), and 50S (lower left). Contour plots of a 1024×1024 subimage are shown on the right; the array center is at [128:128]. The contour intervals are 1×10^{-6} of the peak pixel value of α Ser.

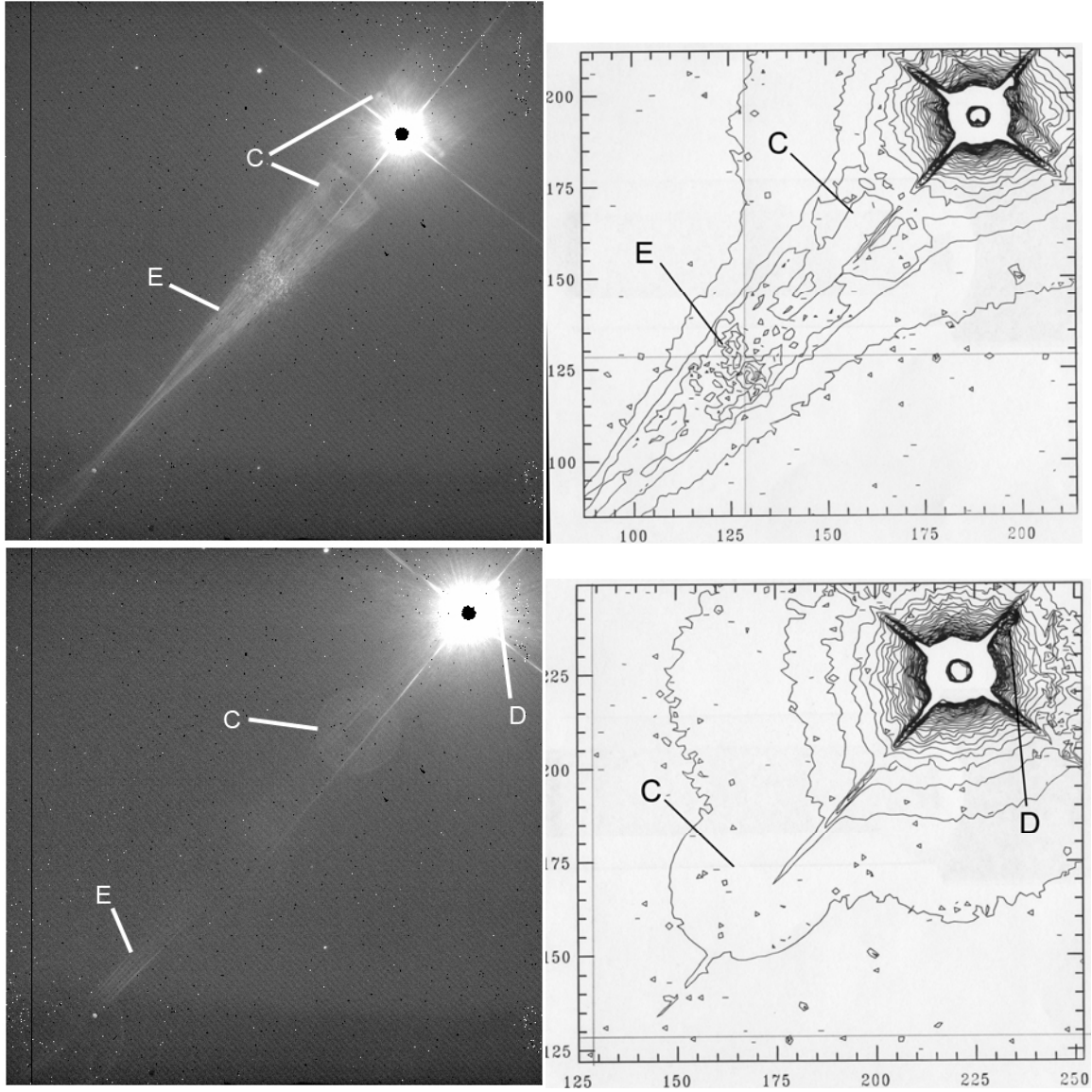


Figure 3: Images of α Ser in the H band 50W50S (upper left), and 75W75S (lower left). Contour plots of a 1024×1024 subimage are shown on the right; the array center is at [128:128]. The contour intervals are 1×10^{-6} of the peak pixel value of α Ser.

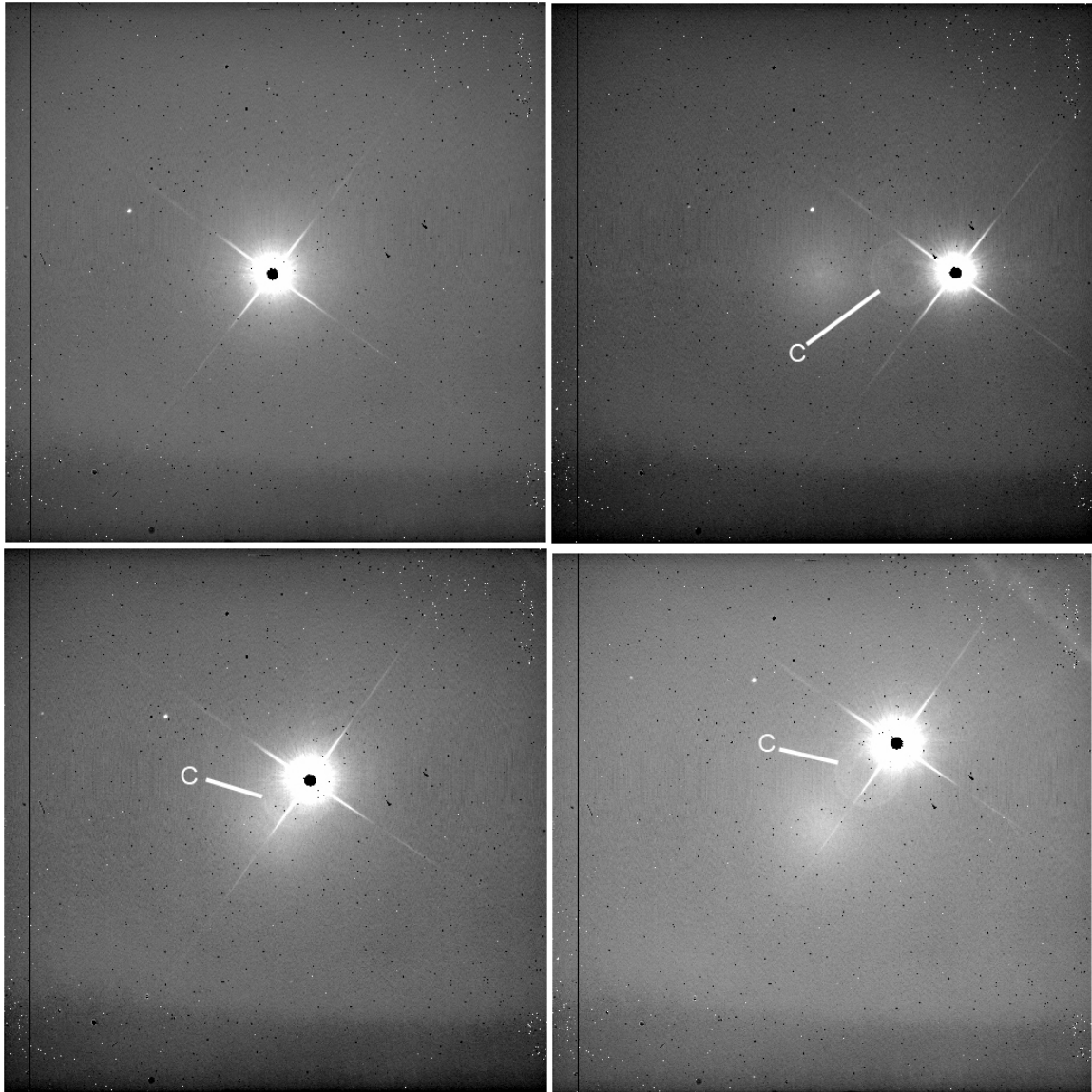


Figure 4: Images of α Ser in the Ks band on-axis (upper left), 50S (upper right), 15W15S (lower left) and 30W30S (lower right). The various ghosts, described in the text, are marked.

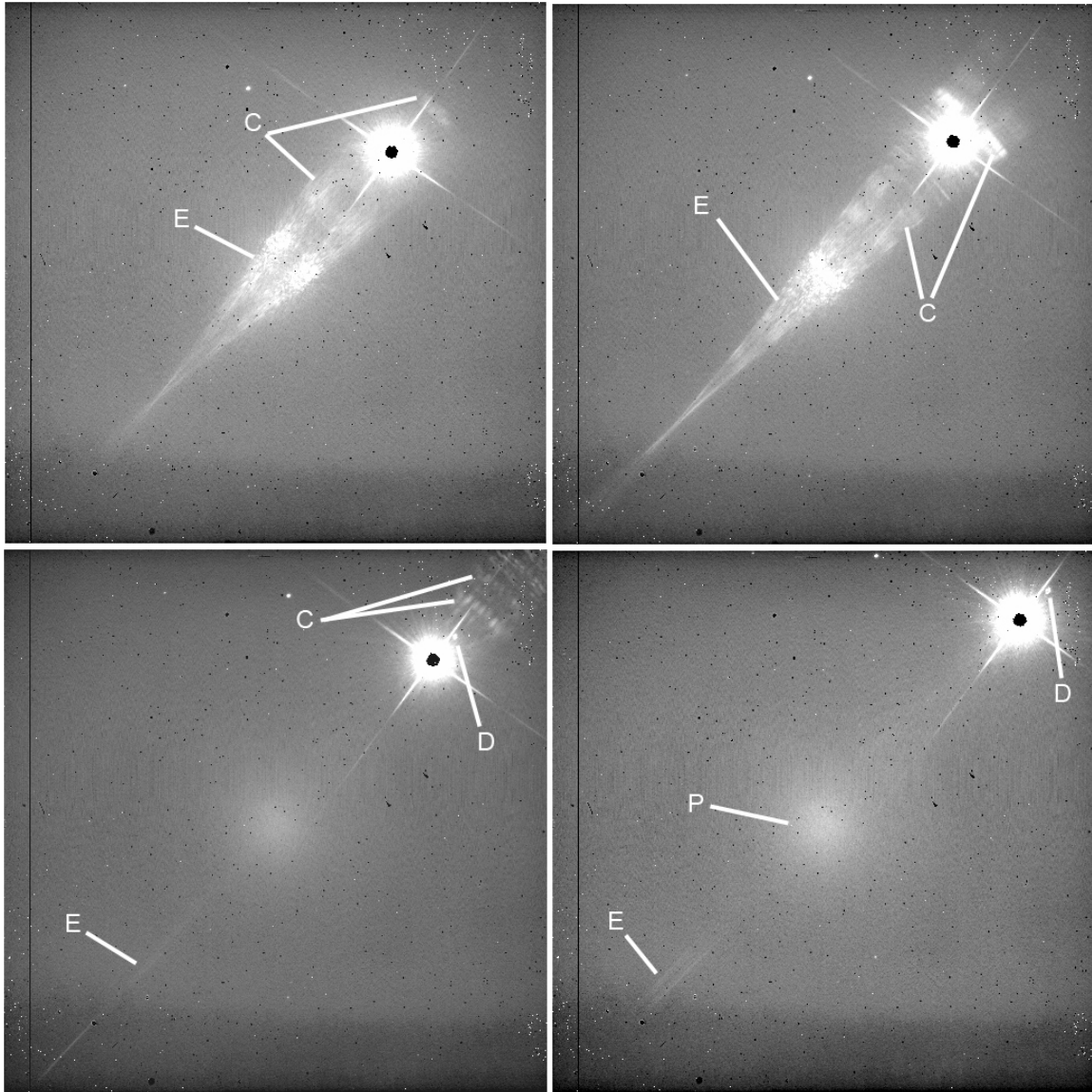


Figure 5: Images of α Ser in the Ks band 45W45S (upper left), 50W50S (upper right), 60W60S (lower left) and 75W75S (lower right). The various ghosts, described in the text, are marked. The ghost marked 'P', which is seen in all of the Ks images, is the pupil ghost.

Ghost Identifications

Several types of ghost images were seen in the data:

- A. A “soft” ghost seen in the on-axis ω Vir image from 15 April, which was also seen only in one image in this series. This is clearly not a ghost, but an afterimage of the initial frame in the series, where the star had been illuminating the array for some time.

- B. A compact ghost seen in off-axis images, halfway between the stellar image and the array center. Almost pointlike (FWHM ~ 7.5 pixels), but slightly kidney-shaped. Seen only in the J and H images, possibly lost in the high Ks sky background noise. Not seen in the images furthest off-axis (75W75S).
- C. A generic series of out-of-focus ghosts along a line between the primary image and the center of the array, seen across the entire array. Several can be seen, but the three most evident are:
- C1: an annular (250 pixels OD; 125 pixels ID) ghost which lies approximately 0.6 of the way between the center of the array and the star, although the ratio decreases with increasing off-axis distance. Typical surface brightness $\sim 1 \times 10^{-6}$ of the stellar peak.
 - C2: two large (~ 500 pixel diameter) ghosts, highly limb-brightened, located on the opposite side of the array at approximately 1.06 and 1.20 times the stellar off-axis distance. Very faint, only edge can be seen at the $\sim 5 \times 10^{-7}$ level.
 - C3: an annular (100 pixels OD; 65 pixels ID) ghost which is seen only in the J band images more than 70 arcsec off-axis at a distance of 0.85 that from the center of the array to the star, at a level $\sim 4 \times 10^{-6}$. Probably masked by scattered light from star for images closer to the optical axis.
- D. Another compact ghost seen in the off-axis images at all wavelengths. This ghost lies along the same line between primary image and the array center, but outside the primary image at a relative distance of 1.14 to the star.
- E. Perhaps less a ghost than a low-intensity streak of scattered light (1×10^{-7}) extending along the primary image – array center axis. However, when the star is approximately 65 – 70 arcsec off-axis, this brightens significantly into a prominent “glint” with additional “arcs” outside of the stellar image. Near the center of the array, this streak exhibits “speckles” which can be quite strong ($\sim 3 \times 10^{-5}$).

Table 1 summarizes the properties of these ghosts. The location of the ghosts lying along the primary image-array center axis is given in terms of R, the distance between the primary image and array center. The peak intensity or surface brightness is relative to the peak pixel intensity of the primary image and the integrated flux relative to the integrated flux of the primary image (these two are nearly the same for the pointlike ghosts).

Table 1: Summary of WHIRC Ghost Images

Type	Description	Location	Peak	Integrated
B	Pointlike, FWHM ~ 7.5 pix	0.5 R	5×10^{-6}	1.7×10^{-5}
C1	Annular, R1 ~ 125 pix; R2 ~ 250 pix	0.60 – 0.45 R	2×10^{-6} (J) 1×10^{-6} (H,K)	2×10^{-3} 2×10^{-3} (H,K)
C2	Annular, R2 ~ 500 pix; only outer edge visible	-1.06 R -1.20 R	5×10^{-7}	
C3	Annular, R1 ~ 65 pix; R2 ~ 100 pix	0.86 R	4×10^{-6} (J)	5×10^{-4} (J)

D	Pointlike, FWHM ~ 8 pix	1.14 R	2×10^{-4} (J) 1×10^{-4} (H) 6×10^{-5} (Ks)	2×10^{-4} (J) 1×10^{-4} (H) 6×10^{-5} (Ks)
E	Streak, 50 – 100 pix wide; bright glint for star 65- 70 arcsec off-axis	Along axis	1×10^{-7} – 3×10^{-5}	

Summary

This brief study of the ghost images in WHIRC is not comprehensive, but allows us to make some conclusions about ghost images seen in source off of the optical axis:

- There are two obvious pointlike ghosts lying along the image-array center axis, at 0.5 and 1.14 of the off-axis distance. In the H band, these ghosts contribute about 1.7×10^{-5} and 1×10^{-4} of the primary source flux, respectively.
- There are a series of defocused, annular ghosts lying along the same axis at various locations. The strongest of these has a surface brightness $\sim 10^{-6}$ of the peak flux of the primary image and an integrated flux $\sim 2 \times 10^{-3}$ of the integrated flux of the primary image.
- There is an additional streak of scattered light along the same axis extending across the entire array, 50 – 100 pixels wide. At the brightest, the surface brightness is $\sim 10^{-7}$ that of the peak of the primary image. The integrated flux is difficult to estimate.
- When the target is approximately 65 – 70 arcsec off-axis, the streak becomes a very prominent wedge-shaped glint extending across the entire array on a line through the array center. Near the center of the array, bright isolated “speckles” appear in the ghost at intensities $\sim 5 \times 10^{-5}$; in addition, bright (3×10^{-5}) arcs appear near the radial location of the star image.
- For some of the ghosts, the intensity tends to be greater at J than at H, almost certainly as a result of the lower AR coating efficiency on the refractive elements and probable higher reflectivity of the detector.
- These ghosts are present in the on-axis image, but are centered on the primary image and impossible to detect separately. The larger annular ghosts blend into the wings of the primary image.

It is instructive to compare these results with those of the ghost modeling presented during the WHIRC CDR. This model considered a total of 13 images, one on-axis, eight at the corners and edges of the array, and four at the half-diagonal locations. The four half-diagonal images did show a pointlike ghost at 1.14 times the off-axis distance, almost certainly the analog of the observed ghost “D”. The calculated ghost/image ratio was 5×10^{-5} , with an estimated integrated flux ratio of 2×10^{-4} , virtually identical to that which we observe at J. Interestingly, the other pointlike ghost “B” did not show up in the model, although at 10 times smaller peak flux, it may have been too faint to be seen in the calculation. The annular “C” ghosts may also have been at too low a level to show up in the model.

The ghost requirement in the acceptance spreadsheet is a relative level no greater than 2×10^{-4} . In terms of integrated flux, the ghost “D”, which is the most intense of the compact ghosts, meets this requirement in the J band and exceeds it in the H band. The annular ghosts exceed this integrated flux level, but the surface brightness is less than the requirement by two orders of magnitude.

The most interesting artifact is the bright glint which appears for a narrow range of target locations. Since the field locations chosen for the ghost analysis were not within this range, this artifact was not predicted. The partial vignetting of the ghost “C1” which is also seen at this location suggests that a reflected beam might be scattering off the edge of a baffle. Despite its impressive appearance, the brightest features are still at a level which meets the acceptance requirements.

Finally, we note that because the reflective ghosts generally appear at fixed ratios of the off-axis field position of the primary target, their relative positions will change during the course of the dithering motions which are a part of the normal observing procedure. They should therefore be amenable to removal during data analysis.